Digest Journal of Nanomaterials and Biostructures Vol. 9, No. 2, April - June 2014, p. 797 - 808

IMPROVING OSSEOINTEGRATION OF ALUMINA/ZIRCONIA CERAMIC IMPLANTS BY FLUORIDE SURFACE TREATMENT

S. CAVALU[a*], C. RATIU[a], O. PONTA[b], V. SIMON[b], D. RUGINA[c], V. MICLAUS[c], I. AKIN[d], G. GOLLER[d]
[a]*University of Oradea, Faculty of Medicine and Pharmacy, Oradea, Romania*
[b]*Babes-Bolyai University, Faculty of Physics & Institute of Interdisciplinary Research inBio-Nano-Sciences, Cluj-Napoca, Romania*
[c]*USAMV, Faculty of Veterinary Medicine, Cluj-Napoca, Romania*
[d]*Istanbul Technical University, Metallurgical and Materials Engineering Department, Turkey*

In the present study, new bioceramic with the composition 75%Al_2O_3-25%3Y-TZP was investigated in vitro and in vivo with the aim of evaluating the osseointegration improvement by surface modification upon SnF_2 and $NaBF_4$ treatment. In vitro tests were carried out in human fibroblasts culture, whereas in vivo tests were performed using an animal model (rabbit). Morphological details of the fibroblasts attached on the surfaces were emphasized by SEM showing the formation of a shell-like coating after 24 hours incubation. Histological images demonstrated the biocompatibility of the treated implants as no gaps, fibrous tissue, multinucleated cells or inflamation were found at the bone implant interface. A better bone to implant contact was noticed in the case of SnF_2 treatment. The results are in agreement with some previously reported studies that also justify the long-term effectiveness of topical fluoride treatment in dentistry and maxillofacial applications.

(Received March 31, 2014; Accepted June 4, 2014)

1. Introduction

By using the ceramic materials in dental restorations and arthroplasty applications since the 70's, a great progress has been recorded along with the tendency of metallic substructure elimination. These materials have a great potential in biomedical field thanks to their biocompatibility, strength, chemical resistance and esthetic properties. Advantages of combined high hardness of alumina with highly fracture resistant yttria stabilized zirconia (YSZ) make Al_2O_3-YSZ system as an alternative choice to alumina and zirconia monolithic ceramics for structural and functional applications. The mechanical properties (hardness and fracture toughness), microstructure and densification with respect to zirconia content and sintering process have been explored previously and reported in some papers [1-6]. Rahaman et al. have reported a comparison of the mechanical properties of some ceramic materials to the Co-Cr alloy and the natural bone, and they have underlined the attractive properties of ceramics, in particular of the ZTA composites [7]. On the other hand, it is mandatory that any material introduced into the human body with the intent to remain there for a long time be tolerated by the organism. Bioinert materials do not release any toxic material but also do not show positive interaction with living tissue. The most common response of the tissue to these materials is formation of a non-adherent fibrous capsule of connective tissue around the bioinert material, and, in the case of bone remodeling, acting like a shape-mediated contact osteogenesis. Through the bone-materials interface only compressive forces will be transmitted („bony on-growth") [8]. Alumina/zirconia bioceramics are most often considered as bioinert materials, but some new formulations and

*Corresponding author: scavalu@uoradea.ro

surface treatments or their constitutive particles may lead to new unexpected biological responses. The influence of surface modifications on the osseointegration of these materials has not been extensively investigated.

The surface characteristics at the micro- or nanometer level, hydrophilicity, biochemical bonding and other features are few of the determiners which are responsible for the implant's success. Osseointegration is not related to certain defined surface characteristics, since a great number of different surfaces achieve osseointegration. The stronger or weaker bone responses may be related to the surface phenomenon and the bone implant interface can be controlled by the selection and modification of the biomaterial from which is made. Hence, many different techniques are currently in use to condition the surfaces of abutments and fixtures of commercially available implants [9]. These include morphological, physiochemical and biochemical methods. The morphological methods involve alterations in the surface morphology and roughness, such as sand blasting, acid etching, fluoride treatments and anodization. The physiochemical methods involve modification of the surface energy, the surface charge and the surface composition by coatings (for example hydroxyapatite coating). The biochemical surface modification goal is to immobilize proteins, enzymes or peptides on biomaterials for the purpose of inducing specific cell and tissue responses, or in other words, to control the tissue-implant interface with molecules which are delivered directly to the interface [10]. In the present study, new bioceramics with the composition 75%Al_2O_3-25%3Y-TZP were investigated in vitro and in vivo with the aim of evaluating the osseointegration improvement by surface modifications upon SnF_2 and $NaBF_4$ treatment. Some previously reported studies also justify the long-term effectiveness of topical fluoride treatment in dentistry and maxillofacial applications [11,12].

2. Experimental

2.1 Preparation of the ceramic specimens and structural characterization:

The starting materials Al_2O_3 (Baikowski grade SM8, an average particle size of 0.6 μm) and 3 mol yttria stabilized ZrO_2 (YSZ, Tosoh grade, an average particle size of 0.1 μm) were used in order to prepare the composite 75%Al_2O_3-25%3Y-TZP by spark plasma sintering method (SPS apparatus SPS-7.40 MK-VII Syntex Inc.). The sintering conditions were 1350° C for 5 min with a heating rate of 100° C/min in vacuum, under a pressure of 40 MPa, as described previously along with the mechanical properties of some different alumina/zirconia composites [2]. Structural characterization of the specimens was made by FTIR spectroscopy (Elmer Perkin BXII spectrometer using KBr pellet technique, resolution of 2 cm^{-1}, at room temperature) and X-ray diffraction analysis carried out with a Shimadzu XRD- 600 diffractometer, using CuKα radiation (λ= 1.5418 Å) with Ni- filter. The morphology of the composite surface (on fracture) was investigated by Scanning Electron Microscopy (FEI Quanta 3D FEG 200/600).

Specimens with conical shape (dimensions: H=8 mm, D=3mm, d=2mm) were manufactured as implants suitable for in vivo tests and respectively discs with D= 10 mm and h=2 mm for cells culture. High purity SnF_2 and $NaBF_4$ (Sigma Aldrich) were used in order to prepare saturated solutions for surface treatment of the specimens by conventional anodization carried out for 2h at 12V. Upon the anodization treatment, the specimens were ultrasonically treated for 90 min to remove the deposits, then air dried. The modifications of samples surface upon both fluoride treatment were investigated by XPS measurements performed with SPECS PHOIBOS 150 MCD system equipped with monochromatic Al-K_α source (250W, hν=1486.64 eV) and E_{pass} = 50 eV, with a resolution of 1 eV/step.

All binding energies were referenced to the C 1s peak arising from adventitious carbon at 284.6 eV and the depth of analysis was about 5 nm. In vitro tests were carried out in human fibroblasts culture, whereas in vivo tests were performed using an animal model (rabbit).

2.2 Cells culture conditions

Human fibroblasts HFL-1 cell line were maintained in a mixture of Dulbecco's Modified Eagle Medium (DMEM) containing 4.5 g/L glucose and Ham's F12 nutrient medium supplemented with 10% fetal bovine serum, 2 mM glutamine, 1% penicilin/streptomicin, 1% non-essential aminoacids at 37°C, 5% CO_2, 95% relative humidity. The upper surfaces of the sterile specimens (discs) were coated with Poly-L-Lysine (Sigma, P4707) for 2h, and then washed with phosphate buffered saline (PBS). A drop (50 μL) containing 5 $*10^4$ HFL-1 cells in culture medium was added on the coated surface of the material for 3h in order to promote cell adhesion. The fixation procedure of the cells attached onto tested material was done after 3, 7 and 24h using paraformaldehyde (4%) for 15 min at room temperature. Three steps of washing using sterile PBS were done prior to the microscopy analysis (SEM and confocal fluorescence). Cell nuclei were counterstained with 5 mM Draq5 diluted 1:1000 in distilled water for 5 min at room temperature. Fluorescent images were acquired with a confocal laser scanning microscope (Zeiss LSM 710), while the morphology of fibroblast cells after 3,7 and 24h incubation time was investigated by SEM (FEI Quanta 3D FEG 200/600).

2.3 In vivo animal model

In a rabbit model, eight animals were selected and ceramic specimens manufactured as conical shape and treated with SnF_2 (n=4) respectively $NaBF_4$ (n=4), were implanted in distal/proximal critical size defect created in the femur. The management of animal husbandry and postoperative care in the vivarium were standardized in-house, as per the guidelines of the Committee for the Purpose of Control and Supervision of Experiments, according to the European legislation and ethics regulations. Radiography of the bone-implant site in the femur was taken after the implantation and before sacrifice. The animals were euthanized at the specific period (6 weeks) and histological analysis were performed in order to detect any immunological or inflammatory responses and to investigate the biological tolerance of the specimens with respect to the bone.

3. Results and discussions

The morphological details of the fractured surfaces of the proposed bioceramic are evidenced in Fig. 1 by SEM micrographs recorded with different magnifications. It has been previously demonstrated that the zirconia addition to alumina matrix promotes composites with higher densities, higher flexural strength and fracture toughness [2, 13]. Alumina grain size as a matrix has an important effect on the hardness and fracture toughness because adding zirconia particles prevent alumina grains from growing to big size.

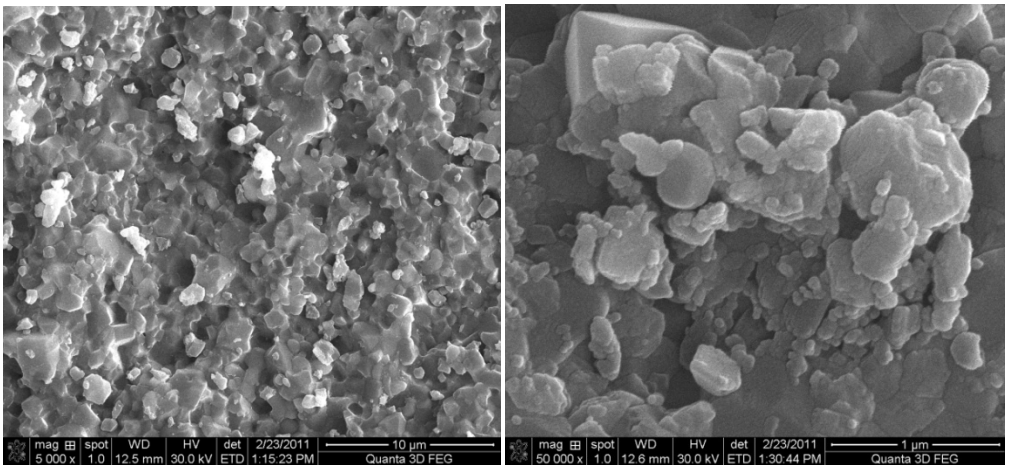

Fig. 1 SEM images showing the morphological details of 75%Al_2O_3-25%3Y-TZP composite.

The structural characterization of the composite, prior to any surface treatment, was performed by FTIR spectroscopy and XRD analysis. The corresponding spectrum and diffractogram are presented in Fig.2 (a,b). The Al-O stretching vibrations of tetrahedral AlO_4 groups are related to the broad, strong band at 1088 cm^{-1} with the shoulder at 1168 cm^{-1}, and to the doublet at 780 and 797 cm^{-1}. The aluminum atoms are differently coordinated, usually by four or six oxygen atoms, and less likely by five oxygens. The absorption bands and shoulders recorded in the spectral region between 465 and 648 cm^{-1} are assigned to six coordinated aluminum and associated with stretching modes of AlO_6 octahedra. The vibrations of Zr-O are visible at 515 and 562 cm^{-1}[14, 15]. XRD patterns of the proposed composite show the characteristics peaks of α-corundum and tetragonal zirconia [16]. The reflection lines occurring from crystallographic planes related to α-corundum are marked at 2θ= 25.6; 35.2; 37.9; 43.4; 57.5; 61.3; 66.4; 68.2; 76.9 and 80.7° while the identification of tetragonal zirconia is assigned to 2θ= 29.9; 49.9; 59.7 and 62.5°. As expected, the constraint exerted by the alumina matrix on the tetragonal zirconia particles maintains them in the tetragonal state.

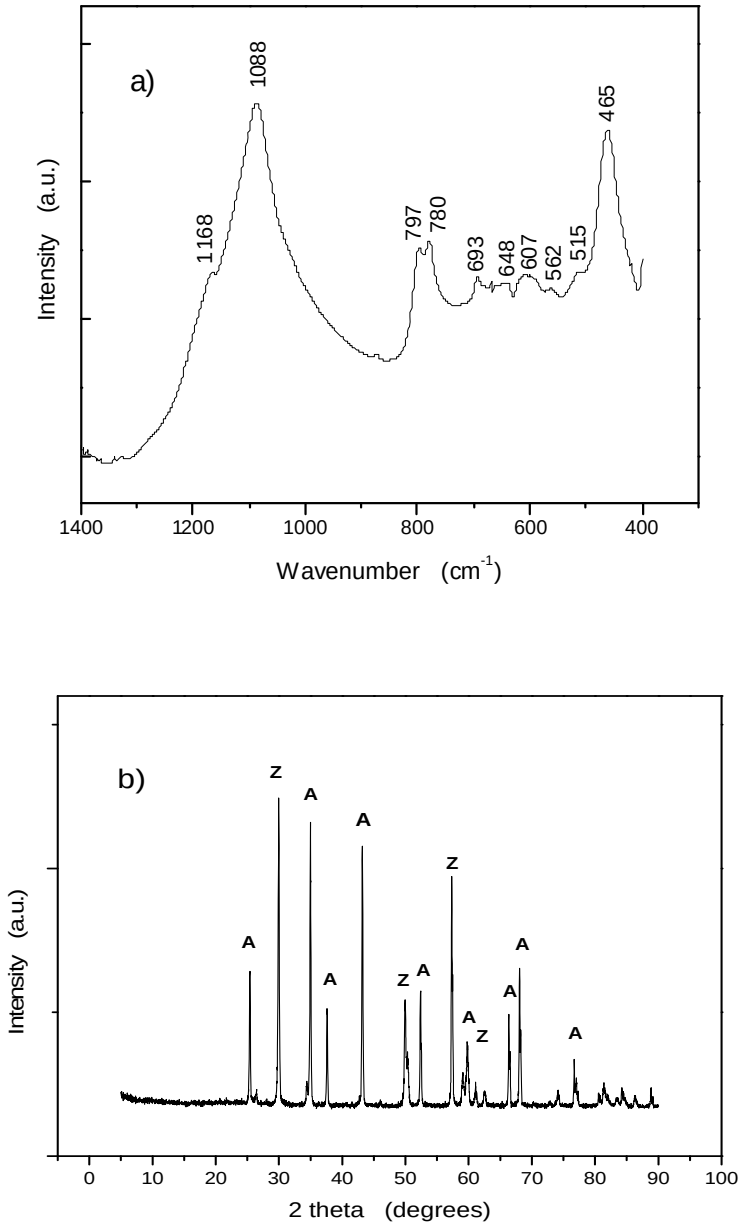

Fig. 2 a) FTIR spectrum and b) XRD pattern of 75%Al_2O_3-25%3Y-TZP composite.

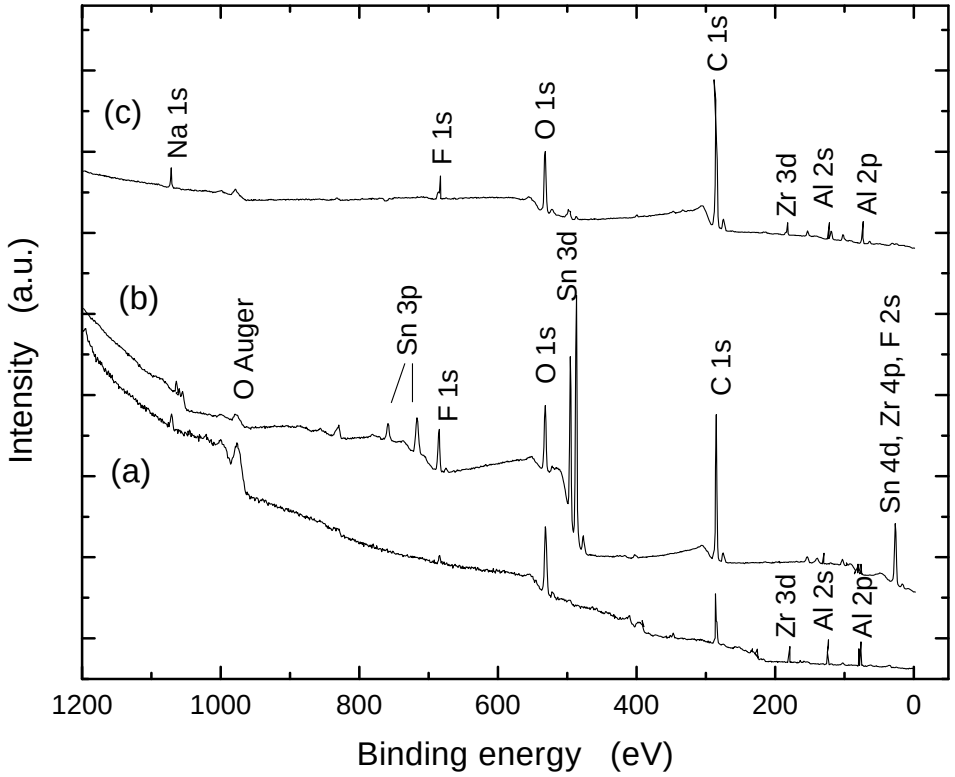

Fig.3 XPS survey spectrum of 75%Al_2O_3-25%3Y-TZP composite before (a) and after treatment with SnF2 (b) and $NaBF_4$ (c) respectively.

As reported in literature [17], XPS analysis is a very sensitive technique demonstrating traces of different chemical components on the implant surfaces after etching, machining, polishing or cleaning processes. In our study, the survey XPS spectra recorded on the surface of the alumina/zirconia ceramic before and after fluoride treatment are presented in Fig. 3. The main photoelectron peaks in the spectra before treatment are assigned to Al 2s (117.9 eV), Al 2p (74.3 eV), O 1s (531.8 eV) and Zr 3d (180 eV). After SnF_2 treatment, a strong Sn $3d_{5/2}$ peak at 487.1 eV indicates the contribution of Sn 3d electrons, while the flour presence is proved by F 1s photoelectrons peak at 685 eV. With respect to the $NaBF_4$ treatment, the marker peaks in this case are F1s at 685.7 eV and Na 1s at 1072 eV, but this treatment shows a less effectiveness compared to SnF_2, as observed by the band intensity. As demonstrated by XPS spectra, the surface of 75%Al_2O_3-25%3Y-TZP composite was strongly affected upon both fluoride treatments.

The optimal surface topography of ceramic implants to promote firm implant- tissue attachment has yet to be determined, as the studies reported in the literature have produced conflicting results, which are not clearly understood. Several in vitro and in vivo studies have demonstrated that the surface structure of ceramic implants influences both the orientation and the proliferation of connective tissue cells and inhibits epithelial downgrowth [9, 18,19]. Thus, before examining the in vivo use of ceramic for bone substitution, we used cultured fibroblasts for the biocompatibility tests. According to the literature, either osteoblasts or fibroblasts could be used, since they are both mesenchymal cells [19-22].

Fig. 4 presents the photographic images of human fibroblasts attached and spread on the surface of alumina/zirconia composite treated with SnF_2 respectively $NaBF_4$. Upon the staining procedure, the visual inspection and photographic images shows the initial stage of attachment at 3h, whereas after 24h, large areas of the surface are covered by the cells layer. By comparing the cells density on the surface, one can observe a better proliferation rate toward the SnF_2 treatment. The fluorescence images recorded with confocal microscope also support this evidence, as presented in Fig. 5. The viable fibroblasts are anchored on both treated surface, showing the evolution of proliferation and colonization capability especially with respect to SnF_2 treatment.

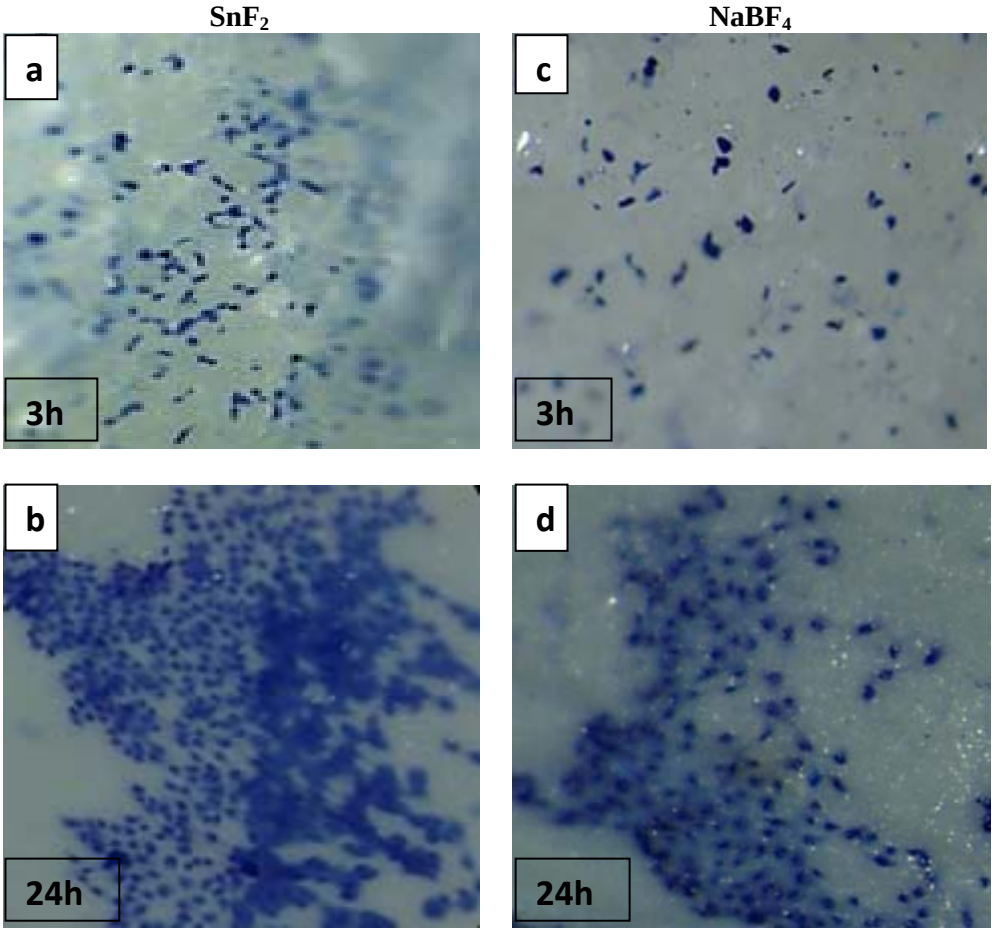

Fig. 4 Photographic images of fibroblasts in different stage of adherence and proliferation to both treated surfaces, after staining procedure: (a,b) 75%Al_2O_3-25%3Y-TZP composite with SnF_2 respectively $NaBF_4$ treatment (c,d).

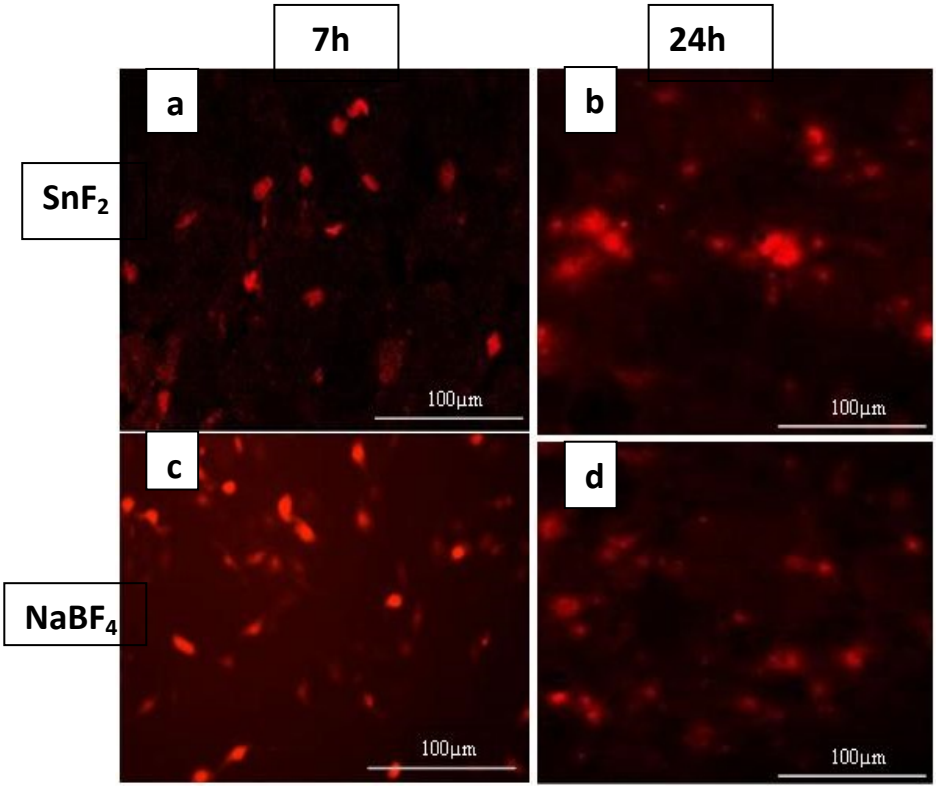

Fig. 5. Fluorescence images of viable fibroblasts attached on the surface of alumina/zirconia composite after SnF_2 (a,b) respectively $NaBF_4$ (c,d) treatment. Results were obtained after 7 and 24 h of culture.

In order to observe the morphology, spreading, orientation and attachment details to each treated surface, the SEM micrographs were recorded at different time intervals and presented in Figs. 6-8. In the first stage, after 3 hours (Fig. 6), the cells did not spread out over the surface, avoiding the contact with the surface treated with SnF_2. By comparison, with respect to the $NaBF_4$ treated surface, the cells are flatted and tend to adhere to the surface. After 7 hours (fig.7) the cells shows numerous filopodia attached to the surface and begin to contact each other in the case of $NaBF_4$ treatment, while spreading out with longer filopodia demonstrating cell attachment and adhesion in the case of SnF2. Cell-to-cell contact suggest possible aggregate formation, since cellular migration is mostly filopodia/lamellipodia dependent [22]. The morphology of cells after 24h indicates a shell-like coating covering a large surface of both treated ceramic material. The cellular layer seems to be more uniform on the $NaBF_4$ treated surface, with well preserved cell-to-cell contact, as presented in Fig. 8 with different details and magnification. However, in both cases, the cells showed a good attachment to the surface, being flat, spread well, conformed intimately to the ceramic surfaces and seemed to form contacts with the adjacent fibroblasts.

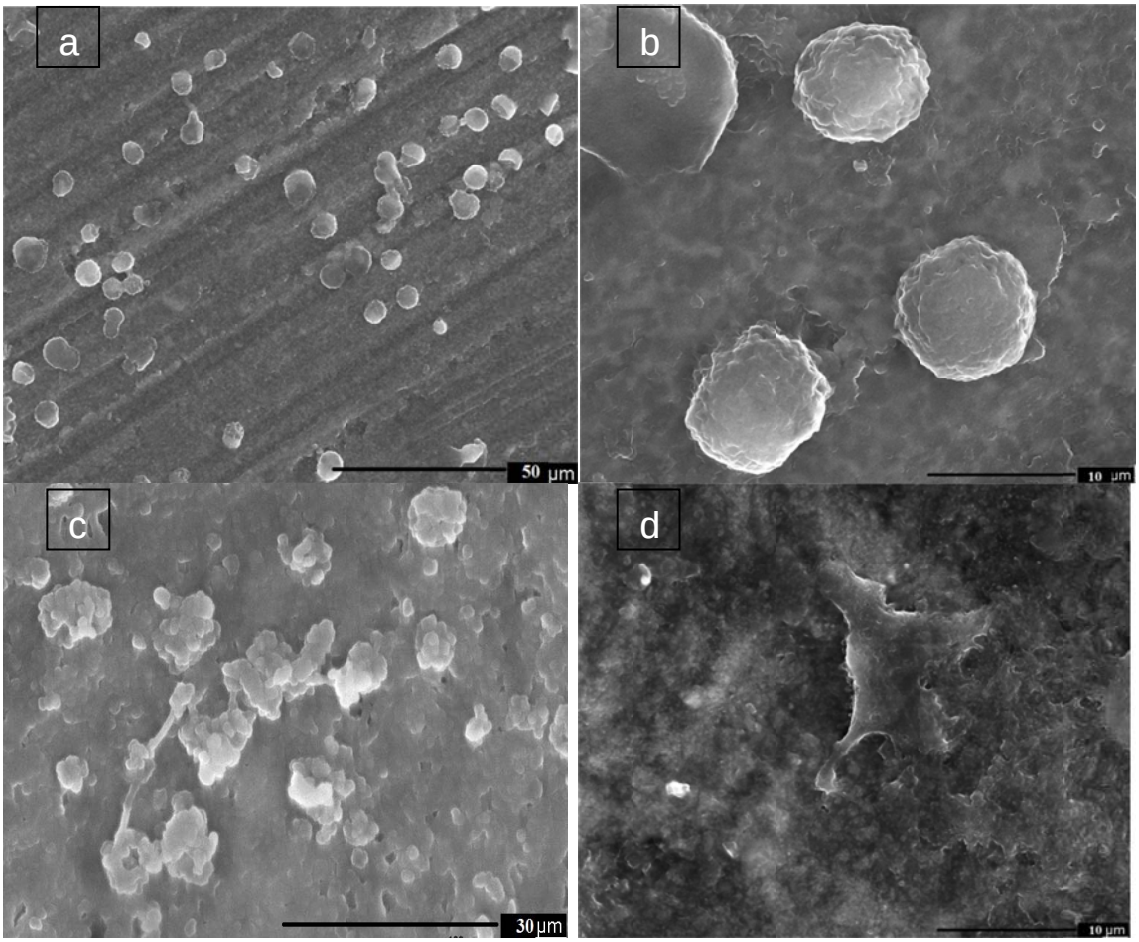

Fig. 6 SEM micrograph showing fibroblasts morphology in contact with the surfaces of alumina/zirconia composite treated with SnF_2 (a,b) respectively $NaBF_4$ (c,d) in the first stage of adherence (3h).

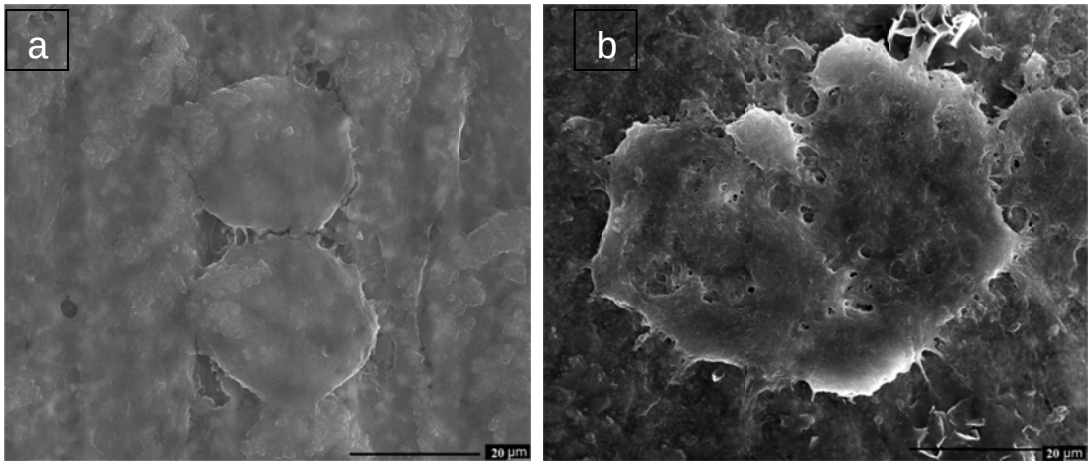

Fig. 7 SEM images of fibroblasts attachment to alumina/zirconia composites treated with NaBF4 (a) respectively SnF2 (b) after 7 hours incubation time.

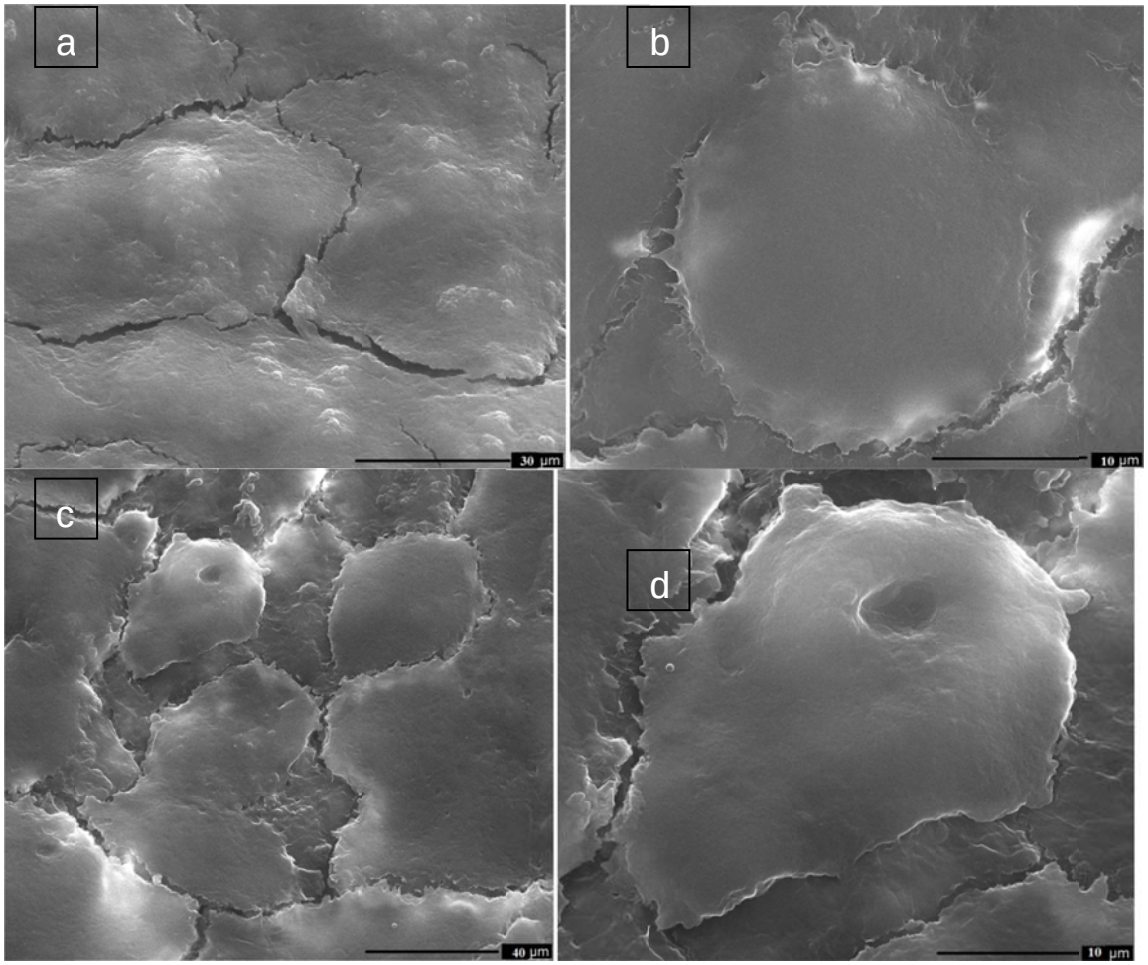

Fig.8 SEM micrographs showing fibroblasts morphology in contact with the surface of alumina/zirconia composite treated with NaBF4 (a,b) respectively SnF2 (c,d) after 24 h incubation time.

It has been demonstrated that animal models allow the evaluation of materials in loaded or unloaded situation over potentially long time duration and in different tissue qualities and ages [23-25]. The main goal of an animal model is to determine whether a new material conforms to the requirements of biocompatibility and mechanical stability prior to clinical use. An ideal bone implant material is defined as having a biocompatible chemical composition, corrosion resistance in the physiologic milieu, acceptable strength, a high resistance to wear and a modulus of elasticity similar to that of bone to minimize bone resorption around the implant. For in vivo tests, the rabbit model has been applied to implant studies because of the availability of proper molecular and cellular biological reagents, as well as its acceptability as a model for the effects of systemic disease on osseointegration. Fig. 9 presents the radiography of the rabbit femur after 2 weeks, along with the photographic image of the defect area after 6 weeks showing a complete coverage with new bone.

Fig. 9 Radiographic image after 2 weeks showing implant insertion and stability in rabbit femur (left). Photographic image showing completely coverage of the defect with new bone after 6 weeks (right).

Histological analysis of the tissue around the implant site was performed by H&E staining for each case and the optical microscopic images are presented in Fig. 10. The general view shows the new bone proliferated toward and above the implant surface in both cases. The newly formed bone surrounded the implant and many osteoblasts secreting osteoid matrix are observed. No gaps or fibrous tissue were present at the interface. No foreign body reaction was found at the bone-implant interface. From visual inspection upon the comparison between the histological images, we can notice a better bone to implant contact in the case of SnF_2 treatment.

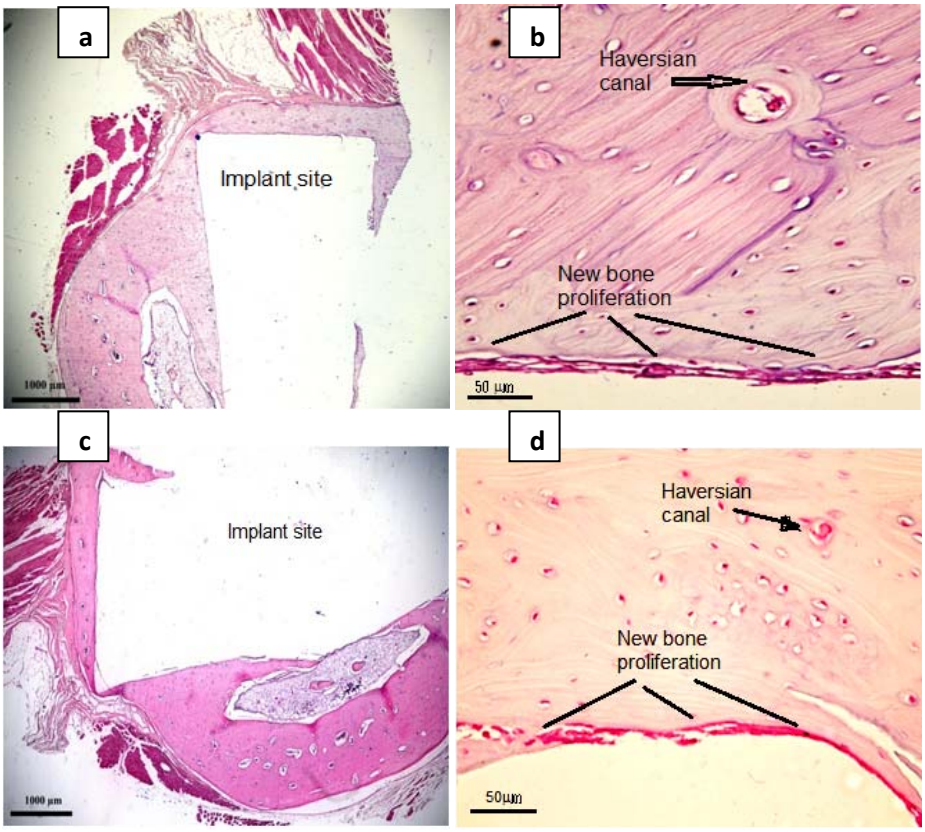

Fig.10 Histological images of the implant surrounding tissue: SnF2 treatment (a,b) respectively NaBF4 treatment (c,d). The images present both general view and details of the newly formed bone in close contact with the implant surface.

4. Conclusions

Our study report the in vitro and in vivo study of new bioceramic with the composition 75%Al_2O_3 25%3YSZ upon surface treatment with SnF_2 and $NaBF_4$. Structural characteristic of the composite was performed by FTIR spectroscopy, XRD analysis and XPS for the evidence of surface modification. Human fibroblasts cells culture in the presence of treated specimens allowed to assay cell adhesion, cell proliferation and colony capability by fluorescence evaluation. Both treatments show similar results, but colonization capability seems to be favored by the SnF_2 treatment. Morphological details of the fibroblasts attached on the surfaces were emphasized by SEM showing the formation of a shell-like coating after 24 hours incubation. From a radiographic and clinical point of view, the tested implants appeared to be osseointegrated. Histological images demonstrated the biocompatibility of the treated implants as no gaps, fibrous tissue, multinucleated cells or inflamation were found at the bone implant interface. A better bone to implant contact was noticed in the case of SnF_2 treatment.

Acknowledgments

This work was accomplished with the support of UEFISCDI**,** project PNII-ID-PCE 2011-3-0441, contract nr. 237/2011. We are grateful to Biochemistry Department of the Oncology Institute "Prof. Dr. Ion Chiricuta" for providing the human fibroblast HFL-1 cell culture.

References

[1] M.C.C.S. Moraes, C.N. Elias, J.D. Filho, L.G. de Oliveira, Mater. Res. **7**, 643 (2004).
[2] I. Akin, E. Yilmaz, F. Sahin, O. Yucel, G. Goller, Ceram. Int. **37**, 3273 (2011).
[3] C. Santos, M.H. Koizumi, J.K.M.F. Daguano, F.A. Santos, C.N. Elias, A.S. Ramos, Mater. Sci. Eng. A **502**, 6 (2009).
[4] M. Arin, G. Goller, J. Vleugels, K. Vammeensel, J. Mater. Sci. 43, 1599 (2008).
[5] A. Navarez-Rascon, A. Aguilar-Elguezabal, E. Orrantia, M. H. Bocanegra-Bernal, Int. J. Refract. Met. Hard Mater. **27**, 962 (2009).
[6] V. Bayazit, M. Bayazit, E. Bayazit, Dig. J. Nanomater. Bios. **7**, 267 (2010).
[7] M.N. Rahaman, A. Yao, B. S. Bal, J.P. Garino, M.D. Ries, J. Am. Ceram. Soc. **90**, 1965 (2007).
[8] L.L. Hench and J. Wilson (Eds), An Introduction to Bioceramics, World Scientific Publishing Co. (1992).
[9] K. Mustafa, A. Wennerberg, K. Arvidson, E. B. Messelt, P. Haag, S. Karlsson, Clin. Oral Impl. Res.**19**, 1178 (2008).
[10] H. Garg, G. Bedi, A. Gargmost, J. Clin. Diagn. Res. **6**, 319 (2012).
[11] S. Cavalu, F. Banica, V. Simon, I. Akin, G. Goller, Int. J. Appl. Ceram Tech **11**, 402 (2014).
[12] F. Lippert, E.E. Newby, R.J. Lynch, V.K. Chauhan, B.R. Schemehorn, J. Clin. Dent. **20**, 45 (2009).
[13] H. Wakily, M. Mehrali, H.S.C. Metselaar, World Acad. Sci. Eng. Tech.**70**, 140 (2010).
[14] C.M. Philippi, K.S. Mazdiyasni, J. Am. Ceram. Soc. **54**, 254 (1971).
[15] D.A. Powers, H.B. Gray, Inorg. Chem.**12**, 2721 (1973).
[16] V. Simon, S. Cavalu, I. Akin, O. Yucel, G. Goller, Studia UBB Physica, **56**, 6 (2011).
[17] G. Mendonca, D.B.S. Mendonca, L.G.P. Simoes, A.L. Araujo, E.R. Leite, W.R. Duarte, J.L. Aragao, L.F. Cooper, Biomaterials **30**, 4053 (2009).
[18] B. Grossner-Schreiber, M. Herzog, J. Hedderich, A. Duck, M. Hannig, M. Greipentrog, Clin. Oral Implants Res. **17**, 736 (2006).
[19] J. Marchi, C. S. Delfino, J. C. Bressiani, H.A. Bressiani, M.M. Marques, Int. J. Appl. Ceram. Technol. **7**, 139 (2010).
[20] O. Roualdes, M.E. Duclos, D. Gutknecht, L. Frappart, J. Chevalier, D. J. Hartmann, Biomaterials **31**, 2043 (2010).

[21] A. Lungu, I. Titorencu, M.G. Albu, N.M. Florea, E. Vasile, H. Iovu, V. Jinga, M. Simionescu, Dig. J. Nanomater. Bios. **6**, 1897 (2011).
[22] N. Saha, A.K.Dubey, B. Basu, J. Biomed. Mater. Res. B, **100B**, 256 (2012).
[23] A.I. Pearce, R.G. Richards, S. Milz, E. Schneider, S.G. Pearce, Eur. Cells Mater.**13**, 1 (2007).
[24] S. Cavalu**,** V.Simon, C. Ratiu, I. Oswald, S.Vlad, O. Ponta, Key Eng. Mater. **583**, 101 (2014).
[25] A. Scarano, F. Di Carlo, M. Quaranta, A. Piattelli, J. Oral Implant. **29**, 8 (2003).